Numerical Simulation of Energy Localization in Dynamic Materials

Mihhail Berezovski and Arkadi Berezovski

Abstract Dynamic materials are artificially constructed in such a way that they may vary their characteristic properties in space or in time, or both, by an appropriate arrangement or control. These controlled changes in time can be provided by the application of an external (non-mechanical) field, or through a phase transition. In principle, all materials change their properties with time, but very slowly and smoothly. Changes in properties of dynamic materials should be realized in a short or quasi-nil time lapse and over a sufficiently large material region. Wave propagation is a characteristic feature for dynamic materials because it is also space and time dependent. As a simple example of the complex behavior of dynamic materials, the one-dimensional elastic wave propagation is studied numerically in periodic structures whose properties (mass density, elasticity) can be switched suddenly in space and in time. It is shown that dynamic materials have the ability to dynamically amplify, tune, and compress initial signals. The thermodynamically consistent high-resolution finite-volume numerical method is applied to the study of the wave propagation in dynamic materials. The extended analysis of the influence of inner reflections on the energy localization in the dynamic materials is presented.

1 Introduction

The wave energy redistribution in materials may result in scattering [1] or harvesting of energy [10]. Such a redistribution can be controlled via the interaction of mechanical waves with a materials microstructure [5]. For instance, unique dynamic properties of phononic crystals can be used to guide and focus elastic waves for

Mihhail Berezovski
Embry Riddle Aeronautical University, Daytona Beach, FL e-mail: mihhail.berezovski@erau.edu

Arkadi Berezovski
Tallinn University of Technology, School of Science, Tallinn, Estonia e-mail: arkadi.berezovski@cs.ioc.ee

wave-based energy harvesting and/or to design materials capable of energy absorbing [4]. Phononic crystals are normally static in the sense that their properties are fixed in advance by their design parameters, which can limit their functionality to very specific arrangements [3]. These constraints appear to limit the usefulness and versatility of phononic crystals to predesigned narrowband operating conditions. Varying the material parameters of the scatterers in the course of time like in dynamic materials (see [6]) will modify the propagation of waves through a phononic crystal. This may enable time-dependent phononic crystals to have more robust or multiple operating regimes as compared to their static counterparts.

The localization of energy during wave propagation is the most intriguing property of dynamic materials [6, 9, 11]. Theoretical analysis of this phenomenon is possible only for zero impedance mismatch [6, 7], which is rarely happens in practice. It is worth, therefore, to study numerically a more general case with non-zero impedance mismatch.

Wave propagation in heterogeneous solids has been a subject of considerable research for many years. However, micro-structural details are rarely taken into account in large-scale structural dynamics or dynamic impact simulations. The reason is the enormous complexity of wave phenomena in highly heterogeneous media. The diversity of possible responses of materials with microstructure to dynamic loading has been recently underlined [12]. This is why the one-dimensional (in space) case is considered.

2 One-dimensional elasticity in small-strain approximation

In general, dynamic materials are characterized by material parameters varying in space and time. In the framework of one-dimensional elasticity, this reflects in the space and time dependence of density ρ and Young's modulus E. With a standard notation (u is the elastic displacement; derivatives indicated by subscripts), the corresponding Lagrangian density has the form [11]

$$L = \frac{1}{2}\rho(x,t)(u_t)^2 - \frac{1}{2}E(x,t)(u_x)^2. \tag{1}$$

The local balance of linear momentum is then written as (no body force for the sake of simplicity)

$$(\rho(x,t)u_t)_t - (E(x,t)u_x)_x = 0. \tag{2}$$

We will consider a situation that may be easier to realize experimentally than the general case, namely, a purely inertial material inhomogeneity ($\rho = \rho(x)$) and only a time evolution of the elasticity coefficient, $E = E(t)$. In this case, we arrive at the wave equation

$$u_{tt} - c^2(x,t)u_{xx} = 0, \tag{3}$$

which can be also represented in the form of the hyperbolic system of the first-order equations

$$v_t = c^2(x,t)\varepsilon_x, \tag{4}$$

$$\varepsilon_t = v_x, \tag{5}$$

where $v = u_t$, $\varepsilon = u_x$, and $c^2(x,t) = E(t)/\rho(x)$.

We will examine the piecewise constant variations in space and time where, in the single space dimension, discontinuities Σ_x are represented by straight lines parallel to the t-axis while discontinuities Σ_t are straight lines parallel to the x-axis (see Figure 1). At the space-like discontinuity surface Σ_x, the continuity of the traction

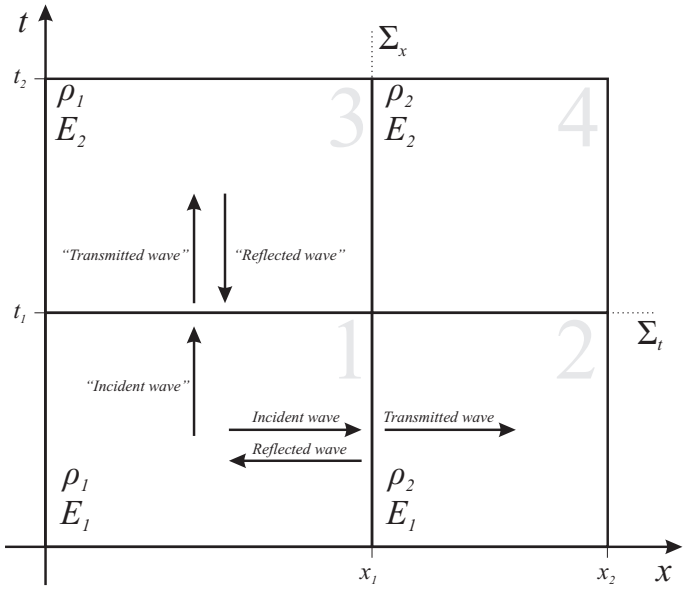

Fig. 1 Propagation diagram (adopted from [8])

is represented as

$$[\![u_x]\!] = 0 \quad \text{at} \quad \Sigma_x, \tag{6}$$

and at the time-like discontinuity surface Σ_t, the continuity of momentum is reduced to [11]

$$[\![u_t]\!] = 0 \quad \text{at} \quad \Sigma_t, \tag{7}$$

where double square brackets denote the usual jump.

The system of equations (4) - (5) with the use of conditions (6) - (7) at fixed discontinuity surfaces is solved numerically by means of the conservative wave-propagation algorithm [2].

3 Numerical simulation of dynamic material behavior

Our goal is to investigate the influence of impedance mismatch, up to 30%, upon the energy localization within the checkerboard structure. We also provide the analysis of the performance of the checkerboard structure for initial disturbance of different lengths (from $\lambda = 100\Delta x$ to $\lambda = 1000\Delta x$). The propagation occurs along 1D medium which can be viewed as an elastic rod. The rod is assumed homogeneous except a region of the length $l = 1000\Delta x$, where dynamic material with a checkerboard structure is maintained (Fig 2.). The homogeneous parts of the rod are used for the better observation of initial and transmitted signals as well as all reflections.

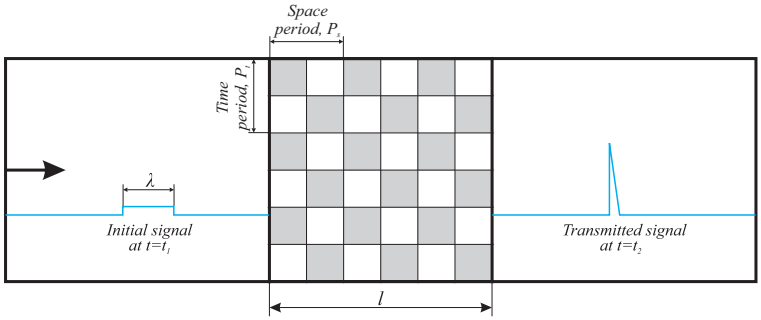

Fig. 2 Geometry of the problem

The checkerboard part consists of a finite number of equal spatial periods with total length of $l = 1000\Delta x$. We consider the case of the checkerboard structure with equal number of steps in time and space periods. The number of time periods is not limited. All the properties are normalized for better comparison of the results, i.e., the elastic velocity c_1 for the fast material is set equal to 1. Through all numerical experiments, we calculate the amplitude of the initial disturbance at time t_1. The amplitude of transmitted signal is measured at time t_2 in the second homogeneous part.

The performance of the checkerboard structure is studied for a range of values of its material parameters, i.e., the elastic velocities c_i and the impedances $z_i = \rho_i c_i$. We also consider the influence of the length λ of the initial disturbance.

All numerical simulations are performed by means of the conservative wave propagation algorithm [2]. This numerical scheme is stable up to the value of the Courant number equal to 1, and second-order accurate on smooth solutions. The typical computational domain is presented in Fig. 3.

Here, the checkerboard structure consists of five space periods of $P_s = 250\Delta x$ each and time periods $P_t = 250\Delta t$. The light blue color represents the fast material with elastic wave velocity $c_1 = 1$. The dark blue represents the slow material, with elastic wave velocity $c_2 = 0.7$. The impedance ratio $z = z_2/z_1$ is set to 1 in this example.

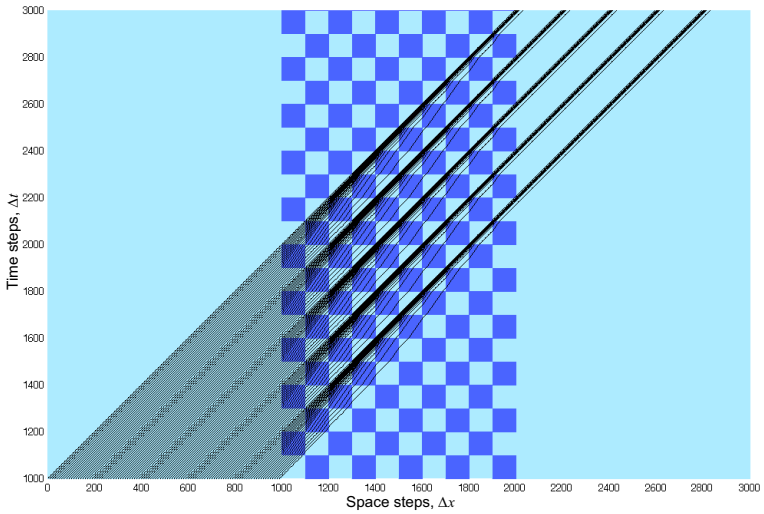

Fig. 3 Computational domain with wave routes ($P_s = 250\Delta x, P_t = 250\Delta t, c_2/c_1 = 0.7, \lambda = 1000\Delta x$)

The black dashed lines represent wave routes for the main disturbance traveling with no reflections (impedance match). We can observe the formation of five limit cycles. It should be noted that this simulation assumes the fixed length and finite numbers of space periods. The corresponding wave field is presented in Fig.4.

The wave field evolution repeats the wave routes behavior. The transformation of the initial pulse into five peaks with higher amplitudes appears due to the limit cycles formation. In this ideal case with equal wave impedances, there is no reflection of waves from the material interfaces.

Our study is focused on the influence produced by a weak impedance mismatch on the energy localization. During the wave propagation through layers with different impedances we expect reflections at the material interfaces. The corresponding wave field history is presented in Fig. 5.

The main peaks of the transmitted signal almost repeat the ideal case with equal impedances (Fig.4). The multiple waves reflected from spatial and temporal interfaces are clearly observed.

4 Amplitude of transmitted pulses

4.1 Amplitude of transmitted pulses vs. velocity ratio

Now we perform simulations varying the elastic wave velocity of the slow material from 0.5 to 1. The length of the initial step pulse is $500\Delta x$ with amplitude equal to

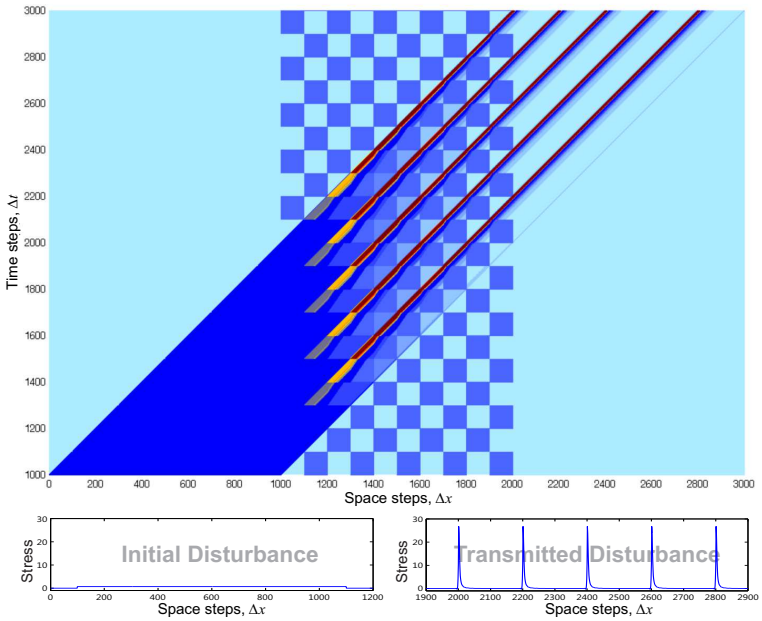

Fig. 4 Wave field time history ($P_s = 250\Delta x, P_t = 250\Delta t, c_2/c_1 = 0.7, \lambda = 1000\Delta x$)

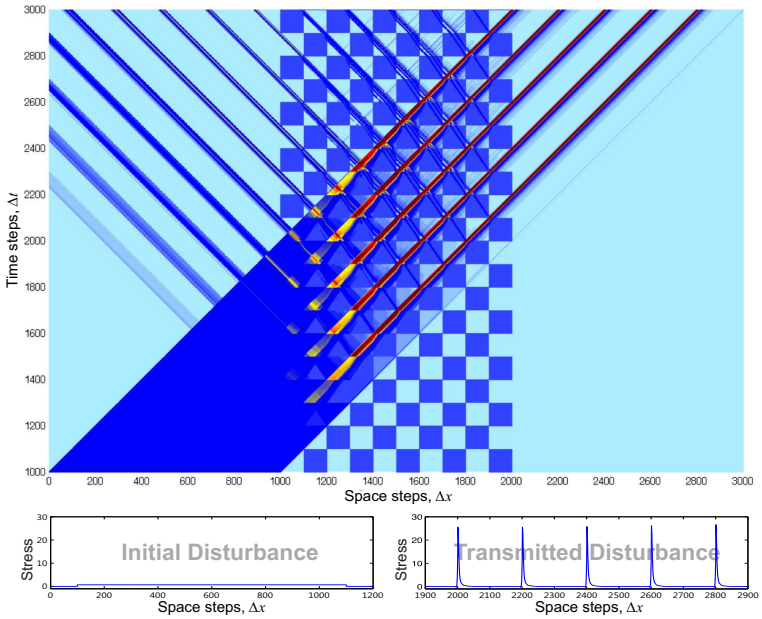

Fig. 5 Wave field time history ($P_s = 250\Delta x, P_t = 250\Delta t, c_2/c_1 = 0.7, z = 0.9, \lambda = 1000\Delta x$)

unity. We repeated these simulations for the impedance ratio mismatch up to 30%. The results are presented in Fig. 6.

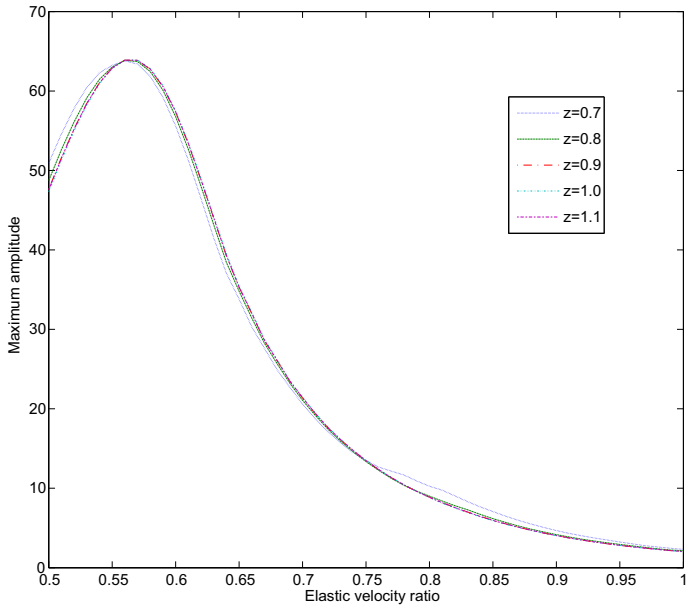

Fig. 6 Amplitude of transmitted pulse vs. elastic velocity ratio for different impedance ratios z ($P_s = 250\Delta x, P_t = 250\Delta t, \lambda = 500\Delta x$)

The normalized amplitude of transmitted pulses is around 50 in the case when the elastic wave velocity in the slow material is two times less than in the fast one for this particular setting. It reaches its maximum for the velocity ratio equal approximately to 0.57. As the elastic wave velocity in slow material becomes closer to that in fast material, the amplitude of transmitted pulses becomes smaller and approaches to that in the initial dispurbance.

These results show that the impedance mismatch up to 30% has very little influence on the amplitude of transmitted pulses. The normalized amplitude plots for different impedance ratios are overlapping each other.

4.2 Amplitude of transmitted pulses vs.wave length

To study the behavior of a checkerboard structure for different lengths of the initial disturbance, we choose the elastic wave velocity ratio equal to 0.7. The length of initial pulse varies from $100\Delta x$ to $1000\Delta x$. The numerical simulations was repeated for impedance ratios z=0.7, 0.8, 0.9, 1.0 and 1.1. The corresponding results are shown in Fig. 7.

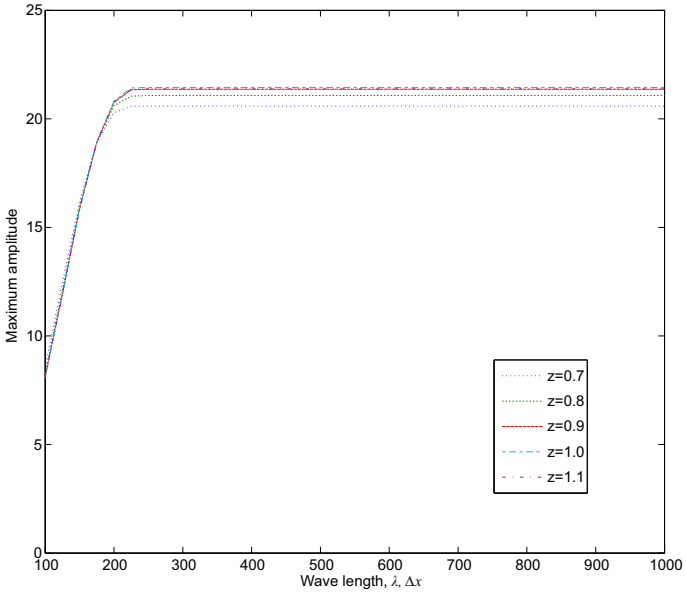

Fig. 7 Amplitude of transmitted pulse vs. wave length for different impedance ratios z ($P_s = 250\Delta x, P_t = 250\Delta t, c_2/c_1 = 0.7$)

It is clearly seen that the amplitude of transmitted pulses for initial signals that are shorter than the length of the space period is increased linearly with the initial wave length. Here the initial disturbance has not enough time to develop into the limit cycles due to the finite number of space periods. As the duration of initial disturbance increases, the amplitude of transmitted pulses becomes constant, because there is a sufficient time to generate well developed limit cycles with the energy localization (see Fig. 3). The average amplitude of transmitted pulses is up to 22. As before, the influence of the impedance mismatch is about 5%.

5 Conclusions

Application of the improved finite volume wave-propagation algorithm [2] allows to implement jump relations both at space-like and time-like discontinuities to simulate wave propagation in dynamic materials. It is shown that dynamic materials demonstrate a very specific transmission of signals. Indeed, the step-wise initial disturbance transforms into a train of localized pulses. The amplitude of such pulses depends on the way of switching material properties of layers, which is external in relation to the wave propagation process. This means that the amplitude of transmitted pulses can be determined only qualitatively. Nevertheless, the influence of parameters of the checkerboard structure on the amplitude of transmitted pulses can

be simulated. As it is shown, the effect of a weak impedance mismatch is small, but the variation of elastic wave velocity ratio is significant. The influence of the length of the initial signal depends on the its ratio to the size of the checkerboard structure.

Acknowledgements Authors appreciate discussions with Prof. G.A.Maugin, Prof. K.A.Lurie, and Prof. S.Weekes. The first author acknowledges the support from Worcester Polytechnic Institute.

References

1. Andreassen, E., Jensen, J.S.: Analysis of phononic bandgap structures with dissipation. Journal of Vibration and Acoustics **135**(4), 041,015 (2013)
2. Berezovski, A., Engelbrecht, J., Maugin, G.A.: Numerical Simulation of Waves and Fronts in Inhomogeneous Solids. World Scientific Singapore (2008)
3. Deymier, P.A., et al.: Acoustic Metamaterials and Phononic Crystals. Springer (2013)
4. Hussein, M.I., Leamy, M.J., Ruzzene, M.: Dynamics of phononic materials and structures: historical origins, recent progress, and future outlook. Applied Mechanics Reviews **66**(4), 040,802 (2014)
5. Le, C., Bruns, T.E., Tortorelli, D.A.: Material microstructure optimization for linear elastodynamic energy wave management. Journal of the Mechanics and Physics of Solids **60**(2), 351–378 (2012)
6. Lurie, K.A.: An Introduction to the Mathematical Theory of Dynamic Materials. Springer (2007)
7. Lurie, K.A., Weekes, S.L.: Wave propagation and energy exchange in a spatio-temporal material composite with rectangular microstructure. Journal of Mathematical Analysis and Applications **314**(1), 286–310 (2006)
8. Maugin, G.A., Rousseau, M.: Prolegomena to studies on dynamic materials and their space-time homogenization. Discrete & Continuous Dynamical Systems-Series S **6**(6), 1599–1608 (2013)
9. Maugin, G.A., Rousseau, M.: Wave Momentum and Quasi-Particles in Physical Acoustics. World Scientific (2015)
10. Radousky, H.B., Liang, H.: Energy harvesting: an integrated view of materials, devices and applications. Nanotechnology **23**(50), 502,001 (2012)
11. Rousseau, M., Maugin, G.A., Berezovski, M.: Elements of study on dynamic materials. Archive of Applied Mechanics **81**(7), 925–942 (2011)
12. Van Pamel, A., Sha, G., Rokhlin, S.I., Lowe, M.J.: Simulation of elastic wave propagation in heterogeneous materials. The Journal of the Acoustical Society of America **141**(5), 3809–3810 (2017)